Integrative Biology

PAPER

Cite this: *Integr. Biol.*, 2017, 9, 135

Zinc sparks induce physiochemical changes in the egg zona pellucida that prevent polyspermy†

Emily L. Que,[a] Francesca E. Duncan,[b] Amanda R. Bayer,[ac] Steven J. Philips,[ad] Eric W. Roth,[ae] Reiner Bleher,[ae] Sophie C. Gleber,[f] Stefan Vogt,[f] Teresa K. Woodruff*[abd] and Thomas V. O'Halloran*[acd]

Received 14th October 2016,
Accepted 7th January 2017

DOI: 10.1039/c6ib00212a

www.rsc.org/ibiology

During fertilization or chemically-induced egg activation, the mouse egg releases billions of zinc atoms in brief bursts known as 'zinc sparks.' The zona pellucida (ZP), a glycoprotein matrix surrounding the egg, is the first structure zinc ions encounter as they diffuse away from the plasma membrane. Following fertilization, the ZP undergoes changes described as 'hardening', which prevent multiple sperm from fertilizing the egg and thereby establish a block to polyspermy. A major event in zona hardening is cleavage of ZP2 proteins by ovastacin; however, the overall physiochemical changes contributing to zona hardening are not well understood. Using X-ray fluorescence microscopy, transmission and scanning electron microscopy, and biological function assays, we tested the hypothesis that zinc release contributes to ZP hardening. We found that the zinc content in the ZP increases by 300% following activation and that zinc exposure modulates the architecture of the ZP matrix. Importantly, zinc-induced structural changes of the ZP have a direct biological consequence; namely, they reduce the ability of sperm to bind to the ZP. These results provide a paradigm-shifting model in which fertilization-induced zinc sparks contribute to the polyspermy block by altering conformations of the ZP matrix. This adds a previously unrecognized factor, namely zinc, to the process of ZP hardening.

Insight, innovation, integration

During fertilization, mammalian eggs exocytose zinc in bursts called zinc sparks. During this process, zinc ions diffuse from the plasma membrane through the zona pellucida (ZP). The ZP glycoprotein matrix serves many functions in the egg and early embryo. During fertilization, the ZP undergoes a hardening process that decreases sperm binding and contributes to the block to polyspermy. Using innovative imaging approaches, we demonstrate that the ZP retains zinc following a zinc spark and this leads to changes in ZP structure. These changes affect ZP function by reducing its ability to bind sperm. These findings establish a novel effect of zinc exocytosis events and demonstrate that zinc efflux is a previously unidentified factor that contributes to the block to polyspermy.

Introduction

The zona pellucida (ZP) is a glycoprotein matrix that surrounds the mammalian egg, and it undergoes a series of structural and functional changes during oogenesis and again later as the egg matures, is fertilized, and transforms into a multicellular embryo.[1,2] During oogenesis, as the egg grows within the ovary, the ZP supports bi-directional communication between the immature egg (also known as an oocyte) and surrounding somatic cells through structures that span the ZP known as transzonal projections.[3,4] Following ovulation of the egg from the ovary, the ZP mediates sperm binding at the time of fertilization.[5] During fertilization, the zona pellucida undergoes partial digestion *via* proteolytic enzymes released from the sperm to allow sperm entry, which is facilitated through interactions between ZP glycoproteins and the sperm head.[6,7] After sperm-egg fusion, the ZP undergoes 'hardening,' which prevents further sperm binding and is referred to as the block to polyspermy.[8–10] Following fertilization and transit of the early embryo through the oviduct and the uterus, the zona pellucida serves as a protective barrier between the developing egg and zygote and the external environment.[10,11]

[a] *The Chemistry of Life Processes Institute, Northwestern University, 2170 North Campus Drive, Silverman 4611, Evanston, IL 60208, USA. E-mail: t-ohalloran@northwestern.edu; Fax: +1-847-467-1566; Tel: +1-847-644-9410*
[b] *Department of Obstetrics and Gynecology, Northwestern University, Feinberg School of Medicine, 303 East Superior Street, Lurie 10-121, Chicago, IL 60611, USA. E-mail: tkw@northwestern.edu; Fax: +1-312-503-0219; Tel: +1-312-503-2503*
[c] *Department of Chemistry, Northwestern University, Evanston, IL 60208, USA*
[d] *Department of Molecular Biosciences, Northwestern University, Evanston, IL 60208, USA*
[e] *Northwestern University Atomic and Nanoscale Characterization Experimental Center, Evanston, IL 60208, USA*
[f] *X-ray Science Division, Argonne National Laboratory, Argonne, IL 60439, USA*
† Electronic supplementary information (ESI) available. See DOI: 10.1039/c6ib00212a

The ZP provides a rigid and defined volume for the dividing zygote as it proceeds through numerous cell divisions during pre-implantation embryo development.[9,10]

Of the various biological functions of the ZP, one 10 of the most important is the block to polyspermy, which would result in an incorrect chromosome complement or aneuploidy. Thus, the polyspermy block is essential because aneuploid zygotes contribute to miscarriages, birth defects, and infertility.[12] The egg has two identified mechanisms for polyspermy prevention: (1) the membrane block that occurs shortly after fertilization and (2) the ZP block known as zona 'hardening'.[8,13–15] The ZP is composed of three glycoproteins—ZP1, ZP2, and ZP3—all of which are essential for maintaining the native three-dimensional structure of the ZP.[11,16,17] ZP2 and ZP3 polymerize into micron-long fibrils that are cross-linked by ZP1 homodimers bridged by a disulfide bond.[18–21] Within minutes of fertilization, membrane bound organelles located at the egg cortex, known as cortical granules, are released by the egg during the cortical reaction. This results in ZP 'hardening,' which prevents polyspermy.[22–25] The term 'hardening' summarizes a number of changes in the ZP following fertilization, including increased resistance to proteolytic digestion,[26] cleavage of the ZP2 protein,[5,27,28] and increased crosslinking (covalent and/or non-covalent) within the ZP protein matrix.[29,30] This transformation is mediated in part by enzymes released during cortical granule exocytosis.[8,30] These enzymes include the zinc-dependent protease ovastacin/SAS1B that cleaves the N-terminus of ZP2, which is essential for sperm recognition.[31–33]

We have established that upon fertilization or after chemical activation (a means of artificially inducing the cellular processes that follow fertilization), the mammalian egg releases zinc in a calcium-coordinated event termed the 'zinc spark.'[34–36] The number of discrete zinc spark events varies from one to five depending upon the type of activation stimulus (sperm, calcium ionophores, $SrCl_2$, PLC-ζ injection, *etc.*) and upon the species (mouse;[34] non-human primate;[34] human[35]). Individual zinc sparks occur over a *ca.* one-minute period and originate from eight thousand of vesicles positioned at the egg cortex, each of which contains an average of one million zinc atoms.[37] Quantitative analysis reveals that the activated egg loses *ca.* 12 billion zinc atoms through these zinc spark events, corresponding to a 20% reduction in the total zinc content of the egg.[38] This loss of intracellular zinc is associated with the inactivation of a zinc-dependent factor that regulates cell cycle resumption inside of the egg, namely EMI2.[39] In fact, when mature eggs arrested in metaphase II (MII) are treated with agents that lower intracellular zinc availability, they activate and reenter the meiotic cell cycle.[34,39,40]

The large-scale translocation of zinc between intracellular compartments and the extracellular environment following activation may play additional roles during egg activation, including ZP hardening. During the zinc spark, the ZP is one of the first structures exposed to the large bolus of exocytosed zinc diffusing away from the egg surface. In addition, the timing of zinc exocytosis is consistent with the timing of ZP hardening.[41] Based on the known amount of zinc lost at the time of fertilization (12 billion atoms), the number of zinc sparks observed (between 1 and 5), and the approximate volume of the zona pellucida region transiently exposed to the zinc spark, we estimate that the zona pellucida is exposed to a zinc concentration in the range of 100 to 500 micromolar during a zinc spark event (see ESI,† Table S1). This zinc level is ten to hundreds of times higher than zinc concentrations observed in follicular fluid, serum, or lymphatic fluid[42,43] and led us to test the hypothesis that these zinc exocytosis events contribute to alterations in the ZP that contribute to its function in blocking sperm binding. Using quantitative elemental analysis, ultrastructural imaging, and sperm binding assays, we show that zinc released during egg activation is retained by and alters the structural properties and biological function of the ZP. These results support an entirely new, functional role for zinc sparks in the block to polyspermy *via* zona hardening in that zinc alone is able to induce structural and functional changes in the ZP in the absence of cortical granule exocytosis or zona protein cleavage. Thus, we can now include zinc efflux as another factor that contributes to the complex process known as ZP hardening.

Materials and methods

Animals, cell collection, and culture

MII eggs were collected from the oviducts of sexually mature (6–10 weeks old) female CD-1 mice injected with 5 IU pregnant mare's serum gonadotropin (PMSG, Sigma-Aldrich) and 5 IU human chorionic gonadotropin (hCG, Sigma-Aldrich) 46 h later. Eggs were isolated from oviducts 14 h after administration of hCG. Collection was performed in Leibovitz's L-15 medium (Life Technologies) supplemented with 1 mg mL^{-1} fetuin (Sigma Aldrich) (L15/fetuin). Cumulus cells were denuded using 0.3% (w/v) hyaluronidase. Parthenotes were obtained by activating MII eggs in 10 mM $SrCl_2$ in Ca-free KSOM (Millipore) for 3 h at 37 °C in an atmosphere of 5% CO_2. Successfully activated cells were selected based on extrusion of the second polar body. Animals were treated in accordance with the US National Institutes of Health Guide for the Care and Use of Laboratory Animals. Food and water were given *ad libitum*. The Northwestern University Institutional Animal Care and Use Committee (IACUC) approved all protocols.

Synchrotron-based X-ray fluorescence microscopy (XFM)

ZPs were isolated from MII eggs and Sr-activated cells using a 50 μm bore Stripper micropipette. Cells were drawn into the pipet and expelled repeatedly in L15/fetuin to separate ZPs and cytoplasm. ZPs were washed through several drops of cytoplasm-free medium, briefly transferred into 100 mM NH_4OAc buffer, and placed on a silicon nitride window (Silson) on a 37 °C heated stage. Buffer was evaporated and additional buffer was used to remove excess salt. XFM was performed at beamline 2-ID-E at the Advanced Photon Source (Argonne National Laboratory, IL). With a single-bounce Si(111) monochromator, 10 keV X-rays were monochromatized and focused to a spot size of 0.5 × 0.6 μm using Fresnel-zone plate optics (X-radia). Fly scans were done in 0.3 μm steps. Fluorescence spectra were collected with a 100 ms dwell time using a silicon drift detector (Vortex-EM). Image analysis

was performed with MAPS software.[44] The fluorescence signal was converted to a two-dimensional concentration in μg cm^{-2} using the thin-film standards NBS-1832 and NBS-1833 (US National Bureau of Standards).

Treatment protocols for comparison of MII, Zn-treated MII, and Sr-activated cells

Following MII collection, cells were divided into separate groups: MII, MII + Zn (50 μM, 500 μM), and Sr-activated cells. MII and MII + Zn groups were treated following one of two protocols. Protocol A (Fig. 2, 3, 4, 5A, and 5B left): the MII group was held in L15/PVP (3 mg mL^{-1} PVP) for 30 min at 37 °C. MII + Zn groups were held in 50 μM or 500 μM $ZnSO_4$. The media pH was neutral in all groups. Protocol B (Fig. 5B right): for MII and MII + 500 μM Zn groups, ZPs were isolated from untreated MII eggs immediately following collection. Isolated ZPs were incubated for 30 min at 37 °C in L15/PVP with and without added Zn.

Electron microscopy

Protocol A was used to prepare MII and MII + Zn samples. Following treatments, cells were collected in methylcellulose capillaries (150 μm inner diameter), fixed (2% paraformaldehyde, 2.5% glutaraldehyde, 0.1 M cacodylate buffer), and post-fixed with 4% osmium tetroxide and 1% uranyl acetate.

Transmission electron microscopy (TEM)

TEM samples were infiltrated with LX-112 resin. Cells were sectioned (50 nm thickness) with a diamond knife on a Leica UC7 ultramicrotome. Sections were stained with 3% uranyl acetate in 50% methanol followed by additional staining with Reynold's lead citrate. Imaging was performed on a Hitachi HT7700 LaB6 TEM at 120 kV.

Scanning electron microscopy (SEM)

SEM samples were critical point dried. Samples were mounted on stubs with carbon tape, and the capillary tubes were carefully cut open to reveal the cells. Cells were further grounded with Ag paint and coated with 5 nm of osmium in a Filgen Osmium Plasma coater. Imaging was performed on a Hitachi SU8030 FE SEM at 3 kV.

Sperm binding assay

MII and MII + Zn eggs were treated following both Protocols A and B, and data from each protocol were analyzed separately. ZPs were isolated using a 50 μm bore Stripper micropipette. ZPs were rinsed through several drops of L15/PVP to remove excess $ZnSO_4$, $SrCl_2$, *etc.* from the media. ZPs were transferred to an IVF dish containing 50 μL drops of TYH/BSA (4 mg mL^{-1}). Equal numbers of ZP were placed in each drop for all groups. During this time, caudal epididymides were collected into L15/PVP from 1 male CD-1 mouse, transferred to TYH/BSA medium, cut, and sperm were allowed to swim out. Sperm were capacitated in TYH/BSA for 1.5 hours at 37 °C and 5% CO_2. Sperm were counted and diluted to 500 000 cells per mL in a 50 μL incubation IVF droplet. After 2 h incubation at 37 °C and 5% CO_2, ZPs were washed (3× in 150 μL L15/PVP drops) and fixed and stained for 30 min with SytoxGreen (1 : 5000 dilution in 950 μL PFA and 50 μL of 20× PBS). Equal number of rinses and transfers were used for each sample. Fixed ZPs were transferred to 5 μL L15 drops on an imaging dish (FluoroDish) and fluorescence was detected using a Leica SP5 confocal and 488 nm laser excitation. Number of sperm bound to each ZP was determined manually using ImageJ.

Statistical analysis

Experimental groups were compared using either a student's *t* test for comparison of two groups or a one-way analysis of variance (ANOVA) for comparison of more than two groups. Statistical tests were performed using the software Prism 5.0 (GraphPad). $p < 0.05$ was considered statistically significant.

Results and discussion

The zona pellucida accumulates zinc following egg activation

To determine if the zinc released during the zinc spark is incorporated into the zona pellucida, we used synchrotron-based X-ray fluorescence microscopy (XFM). This method provides quantitative determination of the total concentration of zinc and additional elements in single ZPs isolated from mature mouse eggs arrested at metaphase II (MII), the meiotic stage during which the gamete is fertilization-competent. We compared the elemental profile of these MII eggs to those that were parthenogenetically activated with $SrCl_2$, a chemical treatment that induces intracellular calcium rises, zinc sparks, and early events of egg activation without sperm (Fig. 1A–C).[34,45] We used parthenogenetically activated eggs instead of eggs fertilized by sperm in order to ensure a uniform activated population of cells given the asynchrony and variability of sperm-mediated fertilization. Following egg activation, the Zn content of the ZP increased significantly by *ca.* 300%, ($p = 0.0138$, Fig. 1D). ZPs isolated from MII eggs contained $3.1 \pm 0.2 \times 10^8$ Zn atoms ($n = 5$), whereas those from activated eggs contained $8.5 \pm 1.7 \times 10^8$ Zn atoms ($n = 5$). Although the sulfur content of the ZP did not change significantly following activation, we did observe a significant increase in the Zn : S mole ratio (Fig. 1E). This suggests that there was an increase in the zinc : protein ratio in the ZP of activated eggs. No changes in copper or calcium levels were observed, but there was a slight decrease in the iron content of the ZP following egg activation (see Table S2, ESI;† $p = 0.0304$). Taken together, these results indicate that egg activation leads to the accumulation of ~5–6 × 10^8 additional zinc atoms or ~1 fmol per ZP. This corresponds to ~5% of the total zinc released from the egg during activation based on previous XFM results.[34]

Zinc exposure does not induce the cortical reaction in MII eggs

A major event at the time of egg activation is the release of cortical granules (CGs) during the cortical reaction. This CG release results in the exocytosis of proteolytic enzymes that modify the ZP and are essential to ZP hardening, including zinc-dependent ovastacin that cleaves the ZP2 protein.[8,30,32] We have further shown that cortical zinc-enriched vesicles release zinc from the egg in concentrated bursts at fertilization.[34,37]

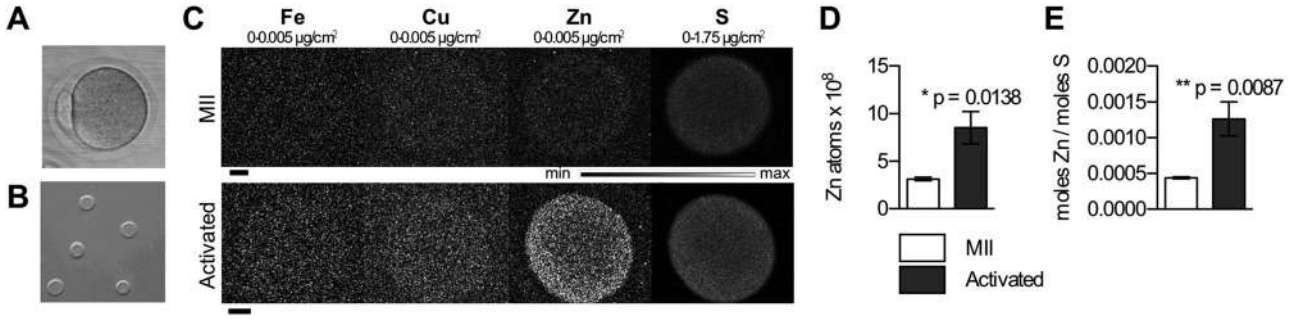

Fig. 1 Zinc accumulates in the zona pellucida (ZP) following egg activation. (A) An intact MII egg, surrounded by the ZP. (B) Isolated ZPs extruded off cells and prepared for X-ray fluorescence microscopy (XFM). (C) Representative Fe, Cu, Zn, and S XFM maps of isolated ZPs prior to (MII) and following (activated) MII egg activation by 10 mM $SrCl_2$. Scale bar, 20 μm. (D) Quantitation of zinc atoms in ZPs from MII (N = 5) and activated (N = 5) cells. (E) Zn : S mole ratio in same samples. Data represents mean values ± s.e.m. (standard error of the mean). The asterisk denotes a statistically significant difference (t test).

Our model system for evaluating the effects of zinc alone on ZP structure and function consists of incubating whole eggs and/or isolated ZPs in exogenous zinc. To exclude the possibility that zinc exposure induces CG exocytosis, we first examined whether eggs exposed to $ZnSO_4$-containing culture media at 50 and 500 μM zinc underwent the cortical reaction in the absence of other activating agents. These concentrations where chosen based on conservative estimates of ZP zinc exposure during a zinc spark (Table S1, ESI†). The distribution of cortical granules was determined in MII eggs, MII eggs treated with Zn, and Sr-activated cells (positive control) using fluorescently labeled Lens Culinaris agglutinin lectin (LCA), an established label for CGs.[46] Projection images from confocal z-stacks are shown in Fig. 2. In eggs arrested at metaphase II (MII), cortical granules are polarized in a hemispherical, cortically enriched distribution (Fig. 2A-i), with the majority of LCA-stained foci present in the vegetal hemisphere (opposite of the chromosomes) of the egg near the plasma membrane, as has been well-described.[30,47] As expected, activation with $SrCl_2$ resulted in a loss of CG density, consistent with what is observed during fertilization (Fig. 2A-iv).[48] Exposure of eggs to exogenous zinc (50 μM and 500 μM) did not alter CG distribution, which remained similar to that of untreated MII eggs (Fig. 2A-ii and iii). Thus, these zinc treatments do not induce cortical granule release in the egg.

We also assessed CG exocytosis status by another standard marker, namely the extent of ZP2 cleavage, which is regulated by the CG enzyme ovastacin.[27,31,32] In Western blot analysis of whole cell lysate from MII eggs, all of the ZP2 protein was in the uncleaved state (120 kDa form), whereas in $SrCl_2$-activated eggs, all the ZP2 protein existed as the 90 kDa cleaved product (Fig. 2B, left). MII eggs treated with 50 μM or 500 μM $ZnSO_4$ contained only the 120 kDa form, indicating that ZP2 cleavage did not occur with zinc treatment. Identical results were obtained when this assay was performed on ZPs isolated from cells following zinc treatments (Fig. 2B, right). This data indicates that the ZP isolation protocol does not subject the ZP to cortical granule components.

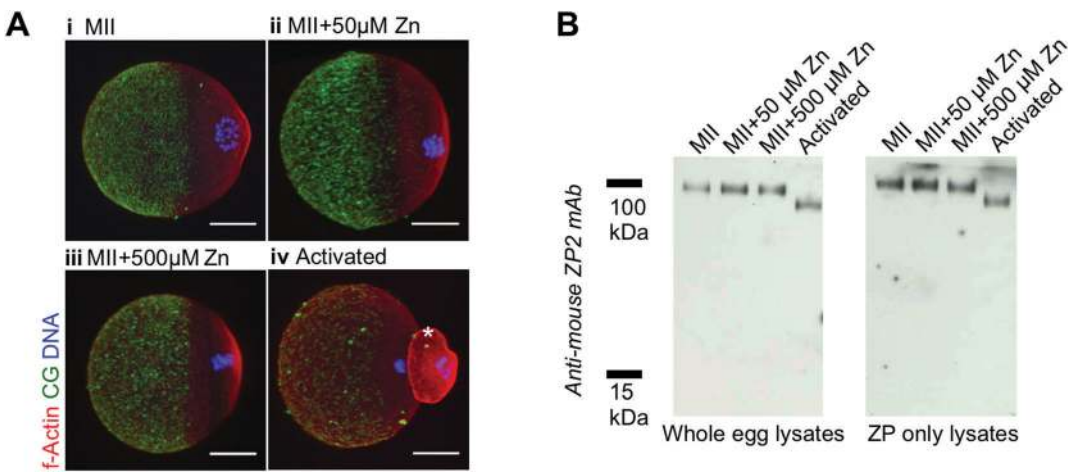

Fig. 2 Zn exposure does not induce the cortical reaction in MII eggs. (A) Representative fluorescence projection images of fixed MII eggs (i), MII eggs treated with 50 μM (ii) and 500 μM $ZnSO_4$ (iii), and parthenotes resulting from Sr activation (iv). Cortical granules (LCA, green), actin (red), and DNA (blue) are shown. Scale bar, 20 μm. Asterisk (*) indicates the second polar body in the activated cell. The first polar bodies were lost during the fixation and staining steps, since the staining was performed with ZP-free eggs. Differences in cell size are due to immunofluorescence processing. All MII samples (i, ii, iii) were the same size prior to fixation and processing. (B) Immunoblots of whole cell (left) and isolated ZP (right) samples probed for ZP2. Ten cells or ZPs were used for each condition to ensure equivalent loading.

In all, these results further support the observation that zinc exposure does not induce the cortical reaction and show that this controlled model system is an effective tool to study the influence of zinc on ZP structure and function independent of CG exocytosis.

Zinc exposure modifies ZP architecture in a manner similar to egg activation

To determine the direct effect of zinc exposure on the structure of the native ZP protein matrix, we used transmission electron microscopy (TEM) and scanning electron microscopy (SEM). These techniques were chosen because of their high resolution and ability to image both internal (TEM) and surface (SEM) structure. These ultrastructural methods have been used previously to characterize the ZPs of mammalian eggs and zygotes and demonstrate increased protein interactions following egg activation.[49–51] ZPs from MII and Sr-activated eggs were compared with ZPs from MII eggs exposed to both 50 μM and 500 μM $ZnSO_4$. In these experiments, zinc treatments were performed on intact eggs.

For the TEM experiments, uranyl acetate was used to highlight protein, membrane, and other biological structures within the specimen, allowing clear visualization of the ZP matrix (Fig. 3A). The ZP protein matrix structure in MII eggs displays large gaps in between stained structures (Fig. 3A-i). Compared to the MII egg, ZPs from $SrCl_2$-activated cells contain fewer gaps within the ZP protein matrix, indicating an increased density of ZP structures following activation (Fig. 3A-iv). A similar increase in density was observed when MII eggs were incubated in both 50 μM and 500 μM $ZnSO_4$ (Fig. 3A-ii and iii respectively). To quantify these observations, we binarized TEM images to separate the ZP structure from the background and calculated the ratio of ZP protein-containing pixels to the total number of pixels in the area covered by the ZP (''pixel ratio'', Fig. 3B; see ESI† for image analysis protocol). The quantitative results demonstrate that the pixel ratio in ZPs from $SrCl_2$-activated cells (0.69 ± 0.09) and ZPs exposed to 50 μM Zn (0.53 ± 0.11) and 500 μM Zn (0.52 ± 0.13) have a significant increase in the observed pixel ratio in TEM images when compared to ZPs from unactivated MII eggs (0.44 ± 0.12, $p = 0.039$). We interpret this ratio change as an increase in the density of the ZP mediated by an increase in interaction between ZP proteins. Indeed, previous work has demonstrated regions of significant condensation in the TEM of ZPs from activated eggs.[50] We note, however, that zinc exposure does not fully recapitulate the morphological changes induced by egg activation, suggesting that zinc exposure is just one mechanism of many that mediates changes in ZP structure.

SEM was also used to more precisely image changes in ZP surface structure following either egg activation or zinc exposure (Fig. 4A). In Fig. 4A-i, analysis of a representative portion of the ZP from an MII egg reveals a network of fibrils, some of which are grouped together into larger fibril bundles (where a fibril bundle is made up of several fibrils). Upon activation (Fig. 4A-iv), the fibrils of the ZP matrix form much larger bundles within the ZP, characterized by greater thickness as indicated by the white brackets. This phenomenon has been previously observed upon activation of bovine eggs.[51] Zinc has a similar effect to activation, with both 50 μM and 500 μM $ZnSO_4$ incubation resulting in thicker bundles within the ZP when compared to MII eggs (Fig. 4A-ii and iii). The average thickness of fibril bundles within these images was quantified using an automated image analysis protocol (see ESI† for details).[52] ZPs from MII eggs had the smallest fibril thickness, averaging 0.19 μm ± 0.08. We observed an increase in ZP fibril thickness after both 50 and 500 μM Zn treatments (0.27 μm ± 0.08 and 0.31 μm ± 0.10), and these increases are indistinguishable from those observed following activation (0.28 μm ± 0.08). All differences were statistically significant relative to the MII group (Fig. 4B, $p = 0.0017$). These results demonstrate that treatment of ZPs with zinc concentrations similar to those observed during

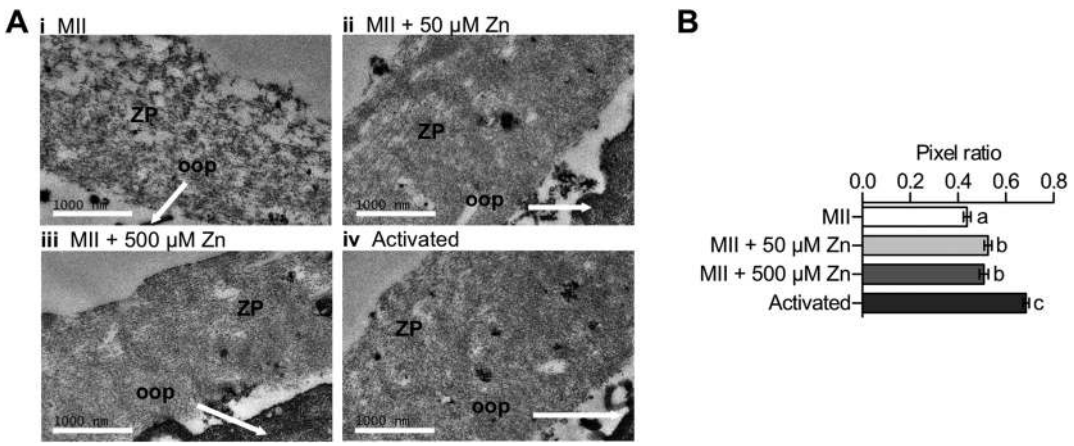

Fig. 3 Zn exposure and activation increase ZP density as shown by transmission electron microscopy (TEM). (A) Representative TEM images of ZP regions from MII eggs (i, $N = 65$), MII eggs treated with 50 μM (ii, $N = 54$) and 500 μM $ZnSO_4$ (iii, $N = 50$), and parthenotes resulting from Sr activation (iv, $N = 46$). The ZP and ooplasm (oop) are indicated in each image. Scale bar, 1000 nm. (B) Pixel ratios determined for different ZP samples. Data represents mean values ± s.e.m. Letters denote statistically significant differences between different sample groups (one-way ANOVA, $p < 0.05$).

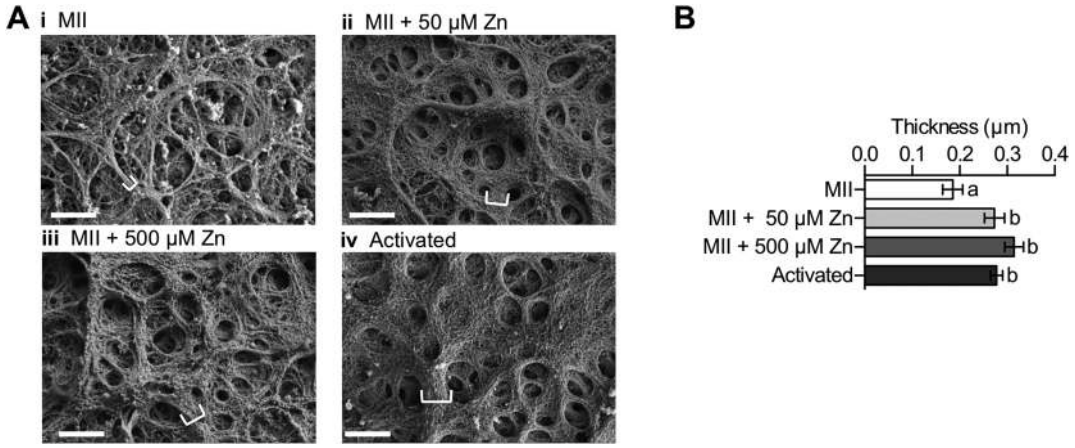

Fig. 4 Zn exposure and activation increase ZP fibril thickness as shown by scanning electron microscopy (SEM). (A) Representative SEM images of MII eggs (i, N = 16), MII eggs treated with 50 μM (ii, N = 27) and 500 μM $ZnSO_4$ (iii, N = 39), and parthenotes resulting from Sr activation (iv, N = 39). White brackets indicate thickness in selected fibril bundles. Scale bar, 1000 nm. (B) Fiber thickness determined for different ZP samples. Data represents mean values ± s.e.m. Letters denote statistically significant differences between different sample groups (one-way ANOVA, $p < 0.05$).

physiological zinc sparks can induce the same type of changes in ZP architecture as those observed in activated eggs.

ZPs exposed to zinc ions have decreased levels of sperm binding

Having demonstrated that the ZP retains zinc following activation and that zinc exposure leads to an altered ZP protein matrix structure, we next examined whether the observed structural changes impacted biological function. An essential role of zona hardening is to block sperm binding to the ZP, thus preventing polyspermy. Therefore, we tested whether ZPs exposed to Zn in the absence of activation would exhibit decreased levels of sperm binding. In these experiments, ZPs from different treatment groups were isolated and incubated with sperm under standard *in vitro* fertilization (IVF) conditions, and the number of bound sperm was quantified using fluorescence microscopy.

In a first set of experiments, intact eggs were incubated in zinc prior to ZP extrusion. ZPs isolated from these samples were compared to ZPs from two control groups: (1) MII eggs incubated without added zinc and (2) $SrCl_2$-activated parthenotes. To avoid any potential effect of unbound zinc on sperm function, excess zinc in the medium was rinsed away from ZP samples prior to the addition of sperm.[53–55] We note that gross morphological analysis showed no obvious difference in sperm number or motility between groups (data not shown). Representative brightfield and fluorescence images (Fig. 5A) reveal that pre-exposure of intact eggs to Zn decreases sperm binding, in much the same way activation does, when compared to the MII control. We used confocal microscopy to quantify the number of sperm bound to each zona in three independent trials (Fig. 5B, left). We found that $SrCl_2$-activated eggs had a significant reduction in sperm-ZP binding (14 ± 16 sperm) when compared to MII controls (110 ± 56, $p < 0.0001$).

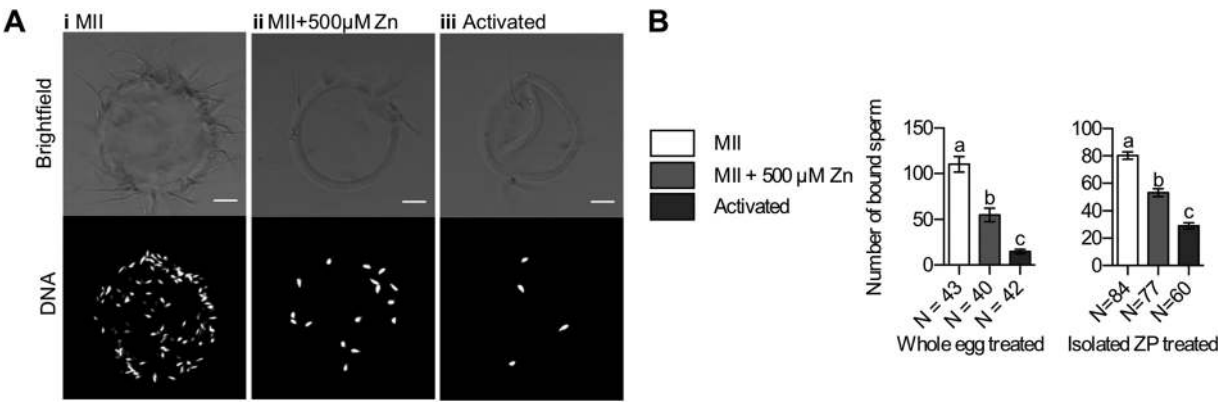

Fig. 5 ZP Zn exposure reduces sperm binding. (A) Representative brightfield (top) and fluorescence images (bottom, DNA) of ZPs isolated from MII eggs (i), MII eggs treated with 500 μM $ZnSO_4$ (ii), and parthenotes resulting from Sr activation (iii). (B) Left: Number of sperm bound to ZP samples in experiments in which whole eggs were treated with zinc. Right: Number of sperm bound to ZP samples in experiments in which isolated ZPs were treated with zinc. Data represents a composite of three separate trials and mean values ± s.e.m. are shown. N values indicate the number of ZPs characterized in each group. Letters denote statistically significant differences between different sample groups (one-way ANOVA, $p < 0.05$).

Furthermore, MII eggs that were incubated in Zn also had fewer bound sperm than the control MII group (55 ± 47, $p < 0.0001$), demonstrating a role for Zn as a modulator of ZP structure and sperm-ZP binding. To further test whether the observed reduction in sperm binding was specifically due to zinc, ZPs were immediately isolated from freshly collected MII eggs prior to incubation with or without zinc. Following incubation, these isolated ZPs were then subjected to the sperm binding assay and compared to ZPs isolated from Sr-activated parthenotes. Showing a similar trend, a significant reduction in sperm binding following zinc incubation (53 ± 24) and activation (29 ± 18) was also observed under these experimental conditions when compared to the MII control (80 ± 25, $p < 0.0001$). These results indicate that the presence of zinc in the ZP reduces sperm binding regardless if the egg cell is present during incubation (Fig. 5B, right). We note that the observed reduction in sperm binding following zinc exposure is not a complete phenocopy of activation, a finding consistent with the previous TEM results. It is likely that exposure to cortical granule enzymes in addition to zinc is required to further reduce sperm binding levels. In all, our data indicates that zinc efflux is one of multiple factors, including ZP2 cleavage by the cortical granule enzyme ovastacin,[5,26,32] that contributes to the modulation of ZP structure and reduction in sperm binding.

Conclusion

The discovery of the zinc spark by our laboratories has prompted a number of studies investigating the roles of zinc flux in the female gamete and early embryo across numerous species.[34–40,56–66] Our estimate of 0.1–0.5 millimolar zinc exposure to the ZP combined with initial zinc release occurring within minutes of fertilization suggested a potential role for the zinc spark in zona pellucida hardening and the block to polyspermy. Herein, we have shown that the ZP accumulates zinc following egg activation, resulting in a tripling of the total zinc content in the ZP as quantified by XFM. Structural proteins of the ZP bind *ca.* 500 million zinc ions, which corresponds to 5% of zinc ions released from cortical vesicles at the time of the zinc spark. While this number is small compared to the total amount of zinc released, our estimates indicate that this amount of zinc (1 fmol) is on par with the amount of glycoprotein monomers present in the ZP (*ca.* 30 fmol), suggesting that zinc is a meaningful component of this extracellular biomaterial. The remaining zinc that is not retained in the zona contributes to the zinc spark phenomenon we have reported[34–37] and may have additional functions including modulating sperm function[67–69] or modifying the oviduct,[70] for example.

Zinc incorporation into the ZP induces a number of structural and physiological changes that resemble those observed in activated egg ZPs. TEM images of ZP cross-sections demonstrated that similar to activation, zinc exposure results in increased density in the ZP, with fewer gaps present in zinc-treated and activated ZPs compared to MII ZPs. SEM images of ZP surfaces illustrated increased fibril aggregation in both zinc-exposed and activated ZPs compared to MII ZPs. Thus, these two electron microscopy methods reveal that zinc exposure to MII ZPs increases the connectivity of the fibrils in this protein matrix both within and on the surface of the ZP. We note that both our TEM and SEM data show that 50 μM and 500 μM zinc treatment yield the same effect, suggesting that only 50 μM zinc is required to crosslink proteins within the ZP. Functionally, exposure of the ZP to Zn reduces the ability of sperm to bind to this glycoprotein matrix, suggesting that zinc released following egg activation is one of the cortically released agents that modifies the function of this biomaterial. Whether zinc-modification of the ZP affects sperm penetration, in addition to sperm binding, is currently under investigation. Taken together, these data suggest that zinc is a key mediator of ZP structure and function and identifies the ZP as a new extracellular target for zinc flux during fertilization and activation. This represents a paradigm shift with regards to zona pellucida hardening, as previously this process was solely attributed to enzymatic factors released during cortical granule exocytosis.[30,32,48] These findings implicate zinc as an important component contributing to ZP hardening that acts independently of CG-derived enzymes. Our TEM and sperm binding data demonstrate that zinc treatment does not fully recapitulate all the changes observed upon egg activation. Thus, multiple mechanisms – including zinc exposure and the action of cortical granule enzymes – are required for complete ZP hardening.

The precise molecular interactions between ZP components and zinc that give rise to fibril bundle formation and the decrease in sperm affinity are currently under investigation. We speculate that zinc ions can coordinate across the polymerized ZP structures that exist in the MII egg, and that these coordination bonds can serve to crosslink ZP fibrils. Previous work in biomaterials suggests that interactions between zinc and metal-binding amino acid residues can significantly affect the structure and properties of macromolecules.[71,72] Tezcan and coworkers have estimated that 4–5% of the characterized protein–protein interfaces in the Protein Data Bank contain a structurally and/or functionally important transition metal cofactor, and zinc is one of the most common of the essential metals found at these interfaces.[73] For example Zn-binding facilitates the formation insulin hexamers, as well as the helical fibrils of the SAM domain of Shank scaffold proteins found in the 'post-synaptic density (PSD)' of excitatory synapses in the brain.[73–75] In these particular cases, zinc release from intracellular vesicles is thought to modulate the structure and function and/or mechanism of the oligomeric proteins outside the cell.

The murine zona pellucida consists of three glycoproteins, ZP1, ZP2, and ZP3. Although all three of these have the potential to act as zinc binding moieties, of these, only ZP3 has available structural data for the full-length protein. ZP3 has many clusters of surface side chains that are capable of forming coordinate covalent bonds with zinc, including His, Asp, and Glu (Fig. S2, ESI†).[76,77] Although surface cysteine residues are tied up in disulfide bonds (and thus are unlikely to participate in metal binding until they are reduced), these clusters of His, Asp and Glu residues in ZP3 are well conserved across several species including mouse, non-human primates, human, bovine, and chicken and that these are situated on the surface of the ZP3 protein (Fig. S2, ESI†). Coordination of zinc to these

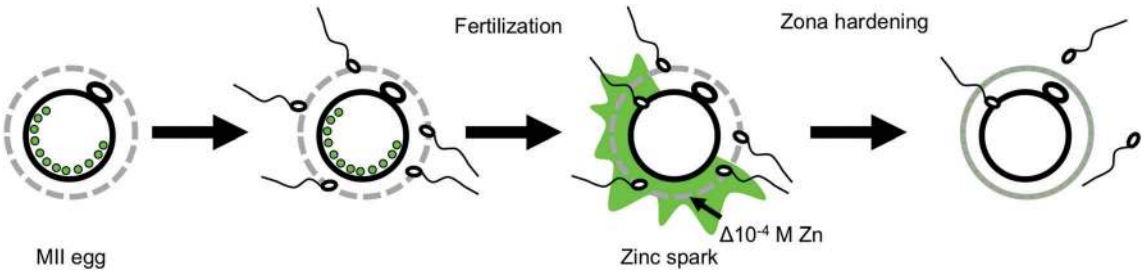

Fig. 6 Schematic of proposed function for extracellular zinc flux during the fertilization-induced zinc spark. Zinc-enriched vesicles in the MII egg are released as zinc sparks following fertilization, exposing the zona pellucida to $\sim 10^{-4}$ M zinc. We propose that this zinc release modifies the structure and function of the zona pellucida to help prevent polyspermy.

ZP3 surface residues would provide a mechanism for forming protein–protein crosslinks within the ZP. We have observed zinc sparks in all of the mammalian species examined to date,[34,35] suggesting that zinc-induced protein crosslinking could be an evolutionarily conserved mechanism for modulating ZP structure and function immediately after fertilization. Zinc-mediated crosslinks could also have roles later in preimplantation embryo development as the embryo travels along the oviduct, enters the mitotic phase, and prepares for implantation.[1,9,78,79] Coordinate covalent bonds formed between zinc and these side chains constitute strong yet labile bonds that can break and reform depending on the stresses placed upon them, giving a dynamic structure that may be necessary for it to adapt to the dividing embryo. Although there is no structural data for ZP1 a structure of the ZP2 ZP-C domain is available.[80] It is possible that metal-binding surface residues on these proteins could participate in Zn^{2+} binding along with those from ZP3. Crystal structures of the full length proteins will enable further investigation into potential zinc binding sites.

These studies demonstrate that zinc treatment induces significant changes in the ZP independently of the enzymes released during the cortical reaction, indicating that elevated zinc concentrations alone can contribute to ZP hardening (Fig. 6). Our results thus provide the first defined molecular role of the zinc spark, *i.e.* transformation of ZP structure and function. The fact that exogenously added zinc only partially phenocopies the physiology of ZP from activated eggs indicates that Zn must work in conjunction with other factors released by the egg to achieve a complete block to sperm binding. It is clear that enzymes released in the cortical reaction must operate in parallel to complete the hardening process. A number of enzymes have been identified as CG components including various hydrolases and a peroxidase.[8,30] Interestingly, ovastacin, found in CGs, is a zinc-dependent metalloprotease that cleaves ZP2 and thus contributes to zona hardening.[31,32] As a result, zinc may have multiple roles during this window of development, acting as a structural ZP component and as an enzymatic cofactor. It is unknown whether ovastacin is loaded with its zinc cofactor before or after the cortical reaction. Thus, whether zinc sparks facilitate loading of zinc into this protease after egg activation remains an open question.

ZP modifications associated with zinc binding and the action of cortical granule enzymes may represent separate but redundant mechanisms that facilitate the block to polyspermy in mammalian eggs. Following fertilization, there are multiple mechanisms that help ensure that only one sperm fertilizes an egg, including processes in the female reproductive tract and processes initiated by the egg itself.[13–15] In the egg, the block to polyspermy occurs *via* mechanisms at both the plasma membrane and the ZP. In mammals, the membrane block to polyspermy occurs during the first 0.5–1 h following fertilization[15] and is mediated by the rapid shedding of the Juno receptor from the egg plasma membrane.[81,82] This receptor interacts with Izumo1, a sperm cell-surface protein, and is essential for sperm-egg binding. ZP hardening mediated by cortical granule enzymes is a slow-acting process, taking >1 h to complete.[15,30,41] Zinc sparks, on the other hand, are initiated almost immediately after fertilization; in fact, in mouse, zinc release from the egg was observed ~ 2 minutes after sperm penetration.[36] Thus, zinc-mediated zona modifications could occur on a much shorter timescale, though the kinetics of this process under fertilization conditions *in vivo* have not yet been investigated. It is likely that all three processes occur within the first hour of fertilization and could represent redundant yet independent mechanisms that the egg uses to ensure monospermic fertilization.

The biological functions of zinc continue to expand from its canonical structural and catalytic roles in metalloproteins to its more recently discovered functions in cell signaling and as a mediator of protein–protein interactions.[73,83–88] The mammalian egg employs temporal and spatial fluctuations in its zinc concentration to regulate a number of distinct mechanisms during the transition from egg to embryo. In the egg, several distinct intracellular zinc fluxes have been found to regulate oocyte maturation and cell cycle progression through the first and second meiotic divisions.[38,39,56,57,65,66] Here, we add an extracellular function for zinc fluxes that are initiated at the time of fertilization. Zinc efflux at this juncture participates in modification of the architecture of the zona pellucida and contributes to the egg's ability to block polyspermy.

Acknowledgements

We thank the Oncofertility Academy programs (https://oncofertility.northwestern.edu/oncofertility-saturday-academies) and science teacher Carole Namowicz and her students from Lindblom Math and Science Academy (Chicago, IL) for help with XFM

experiments, Jurrien Dean for providing us with ZP2 antibody, and Luca Jovine for discussions of ZP3 structural data. Electron microscopy was performed in the EPIC facility (NU*ANCE* Center-Northwestern University), which has received support from the MRSEC program (NSF DMR-1121262) at the Materials Research Center; the International Institute for Nanotechnology (IIN); and the State of Illinois, through the IIN. This work was supported by a Medical Research Award from the W. M. Keck Foundation, the Chemistry of Life Processes Cornew Innovation Fund a SPARK Award from the Chicago Biomedical Consortium, and the National Institutes of Health (P01 HD021921, GM38784, GM115848, GM038784, U54P50HD076188, and T32GM105538). This research used resources of the Advanced Photon Source, a U.S. Department of Energy (DOE) Office of Science User Facility operated for the DOE Office of Science by Argonne National Laboratory under Contract No. DE-AC02-06CH11357.

References

1 J. A. Modlinski, *J. Embryol. Exp. Morphol.*, 1970, **23**, 539–547.
2 T. Rankin, S. Soyal and J. Dean, *Mol. Cell. Endocrinol.*, 2000, **163**, 21–25.
3 D. F. Albertini, C. M. Combelles, E. Benecchi and M. J. Carabatsos, *Reproduction*, 2001, **121**, 647–653.
4 D. F. Albertini and V. Rider, *Microsc. Res. Tech.*, 1994, **27**, 125–133.
5 J. D. Bleil, C. F. Beall and P. M. Wassarman, *Dev. Biol.*, 1981, **86**, 189–197.
6 A. Abou-Haila and D. R. Tulsiani, *Arch. Biochem. Biophys.*, 2000, **379**, 173–182.
7 P. Morales, N. L. Cross, J. W. Overstreet and F. W. Hanson, *Dev. Biol.*, 1989, **133**, 385–392.
8 Q. Y. Sun, *Microsc. Res. Tech.*, 2003, **61**, 342–348.
9 P. M. Wassarman, *J. Biol. Chem.*, 2008, **283**, 24285–24289.
10 P. M. Wassarman and E. S. Litscher, *Int. J. Dev. Biol.*, 2012, **56**, 833–839.
11 T. Rankin, P. Talbot, E. Lee and J. Dean, *Development*, 1999, **126**, 3847–3855.
12 T. Hassold and P. Hunt, *Nat. Rev. Genet.*, 2001, **2**, 280–291.
13 P. Coy and M. Aviles, *Biol. Rev. Cambridge Philos. Soc.*, 2010, **85**, 593–605.
14 B. Dale and L. DeFelice, *J. Assist. Reprod. Genet.*, 2011, **28**, 199–207.
15 A. J. Gardner and J. P. Evans, *Reprod., Fertil. Dev.*, 2006, **18**, 53–61.
16 T. Rankin, M. Familari, E. Lee, A. Ginsberg, N. Dwyer, J. Blanchette-Mackie, J. Drago, H. Westphal and J. Dean, *Development*, 1996, **122**, 2903–2910.
17 T. L. Rankin, M. O'Brien, E. Lee, K. Wigglesworth, J. Eppig and J. Dean, *Development*, 2001, **128**, 1119–1126.
18 J. M. Greve and P. M. Wassarman, *J. Mol. Biol.*, 1985, **181**, 253–264.
19 M. Monne and L. Jovine, *Biol. Reprod.*, 2011, **85**, 661–669.
20 P. M. Wassarman, *Cell*, 1999, **96**, 175–183.
21 H. Okumura, T. Sato, R. Sakuma, H. Fukushima, T. Matsuda and M. Ujita, *FEBS Open Bio*, 2015, **5**, 454–465.
22 T. Ducibella, *Hum. Reprod. Update*, 1996, **2**, 29–42.
23 D. Kline and J. Stewart-Savage, *Dev. Biol.*, 1994, **162**, 277–287.
24 S. H. Lee, K. K. Ahuja, D. J. Gilburt and D. G. Whittingham, *Development*, 1988, **102**, 595–604.
25 J. Stewart-Savage and B. D. Bavister, *Mol. Reprod. Dev.*, 1991, **30**, 390–395.
26 A. C. Schroeder, R. M. Schultz, G. S. Kopf, F. R. Taylor, R. B. Becker and J. J. Eppig, *Biol. Reprod.*, 1990, **43**, 891–897.
27 T. L. Rankin, J. S. Coleman, O. Epifano, T. Hoodbhoy, S. G. Turner, P. E. Castle, E. Lee, R. Gore-Langton and J. Dean, *Dev. Cell*, 2003, **5**, 33–43.
28 G. Gahlay, L. Gauthier, B. Baibakov, O. Epifano and J. Dean, *Science*, 2010, **329**, 216–219.
29 D. P. Green, *Rev. Reprod.*, 1997, **2**, 147–156.
30 T. Hoodbhoy and P. Talbot, *Mol. Reprod. Dev.*, 1994, **39**, 439–448.
31 V. Quesada, L. M. Sanchez, J. Alvarez and C. Lopez-Otin, *J. Biol. Chem.*, 2004, **279**, 26627–26634.
32 A. D. Burkart, B. Xiong, B. Baibakov, M. Jimenez-Movilla and J. Dean, *J. Cell Biol.*, 2012, **197**, 37–44.
33 M. Sachdev, A. Mandal, S. Mulders, L. C. Digilio, S. Panneerdoss, V. Suryavathi, E. Pires, K. L. Klotz, L. Hermens, M. B. Herrero, C. J. Flickinger, M. van Duin and J. C. Herr, *Dev. Biol.*, 2012, **363**, 40–51.
34 A. M. Kim, M. L. Bernhardt, B. Y. Kong, R. W. Ahn, S. Vogt, T. K. Woodruff and T. V. O'Halloran, *ACS Chem. Biol.*, 2011, **6**, 716–723.
35 F. E. Duncan, E. L. Que, N. Zhang, E. C. Feinberg, T. V. O'Halloran and T. K. Woodruff, *Sci. Rep.*, 2016, **6**, 24737.
36 N. Zhang, F. E. Duncan, E. L. Que, T. V. O'Halloran and T. K. Woodruff, *Sci. Rep.*, 2016, **6**, 22772.
37 E. L. Que, R. Bleher, F. E. Duncan, B. Y. Kong, S. C. Gleber, S. Vogt, S. Chen, S. A. Garwin, A. R. Bayer, V. P. Dravid, T. K. Woodruff and T. V. O'Halloran, *Nat. Chem.*, 2015, **7**, 130–139.
38 A. M. Kim, S. Vogt, T. V. O'Halloran and T. K. Woodruff, *Nat. Chem. Biol.*, 2010, **6**, 674–681.
39 M. L. Bernhardt, B. Y. Kong, A. M. Kim, T. V. O'Halloran and T. K. Woodruff, *Biol. Reprod.*, 2012, **86**, 114.
40 T. Suzuki, N. Yoshida, E. Suzuki, E. Okuda and A. C. Perry, *Development*, 2010, **137**, 2659–2669.
41 M. Inoue and D. P. Wolf, *Biol. Reprod.*, 1975, **13**, 546–551.
42 Y. Menezo, L. Pluntz, J. Chouteau, T. Gurgan, A. Demirol, A. Dalleac and M. Benkhalifa, *Reprod. Biomed. Online*, 2011, **22**, 647–652.
43 S. C. Ng, R. Karunanithy, W. R. Edirisinghe, A. C. Roy, P. C. Wong and S. S. Ratnam, *Gynecol. Obstet. Invest.*, 1987, **23**, 129–132.
44 S. Vogt, *J. Phys. IV*, 2003, **104**, 635–638.
45 S. F. Ma, X. Y. Liu, D. Q. Miao, Z. B. Han, X. Zhang, Y. L. Miao, R. Yanagimachi and J. H. Tan, *Theriogenology*, 2005, **64**, 1142–1157.
46 G. N. Cherr, E. Z. Drobnis and D. F. Katz, *J. Exp. Zool.*, 1988, **246**, 81–93.
47 T. Ducibella, E. Anderson, D. F. Albertini, J. Aalberg and S. Rangarajan, *Dev. Biol.*, 1988, **130**, 184–197.

48 A. L. Abbott and T. Ducibella, *Front. Biosci.*, 2001, **6**, D792–806.
49 G. Familiari, R. Heyn, M. Relucenti and H. Sathananthan, *Front. Biosci.*, 2008, **13**, 6730–6751.
50 G. Familiari, S. A. Nottola, G. Macchiarelli, G. Micara, C. Aragona and P. M. Motta, *Mol. Reprod. Dev.*, 1992, **32**, 51–61.
51 H. Suzuki, J. C. Ju and X. Yang, *Cloning*, 2000, **2**, 69–78.
52 M. Doube, M. M. Klosowski, I. Arganda-Carreras, F. P. Cordelieres, R. P. Dougherty, J. S. Jackson, B. Schmid, J. R. Hutchinson and S. J. Shefelbine, *Bone*, 2010, **47**, 1076–1079.
53 J. C. Andrews, J. P. Nolan, R. H. Hammerstedt and B. D. Bavister, *Biol. Reprod.*, 1994, **51**, 1238–1247.
54 C. Foresta, A. Garolla, I. Cosci, M. Menegazzo, M. Ferigo, V. Gandin and L. De Toni, *Hum. Reprod.*, 2014, **29**, 1134–1145.
55 M. Hidiroglou and J. E. Knipfel, *J. Dairy Sci.*, 1984, **67**, 1147–1156.
56 B. Y. Kong, M. L. Bernhardt, A. M. Kim, T. V. O'Halloran and T. K. Woodruff, *Biol. Reprod.*, 2012, **87**(11), 11–12.
57 B. Y. Kong, F. E. Duncan, E. L. Que, A. M. Kim, T. V. O'Halloran and T. K. Woodruff, *Mol. Hum. Reprod.*, 2014, **20**, 1077–1089.
58 B. Y. Kong, F. E. Duncan, E. L. Que, Y. Xu, S. Vogt, T. V. O'Halloran and T. K. Woodruff, *Dev. Dyn.*, 2015, **244**, 935–947.
59 X. Tian, K. Anthony, T. Neuberger and F. J. Diaz, *Biol. Reprod.*, 2014, **90**, 83.
60 Y. Jeon, J. D. Yoon, L. Cai, S. U. Hwang, E. Kim, Z. Zheng, E. Jeung, E. Lee and S. H. Hyun, *Mol. Med. Rep.*, 2015, **12**, 5973–5982.
61 Y. Jeon, J. D. Yoon, L. Cai, S. U. Hwang, E. Kim, Z. Zheng, E. Lee, D. Y. Kim and S. H. Hyun, *Theriogenology*, 2014, **82**, 866–874.
62 K. Lee, A. Davis, L. Zhang, J. Ryu, L. D. Spate, K. W. Park, M. S. Samuel, E. M. Walters, C. N. Murphy, Z. Machaty and R. S. Prather, *Theriogenology*, 2015, **84**, 1024–1032.
63 M. H. Zhao, N. H. Kim and X. S. Cui, *In Vitro Cell. Dev. Biol.: Anim.*, 2014, **50**, 945–951.
64 M. H. Zhao, J. W. Kwon, S. Liang, S. H. Kim, Y. H. Li, J. S. Oh, N. H. Kim and X. S. Cui, *PLoS One*, 2014, **9**, e102097.
65 X. Tian and F. J. Diaz, *Endocrinology*, 2012, **153**, 873–886.
66 X. Tian and F. J. Diaz, *Dev. Biol.*, 2013, **376**, 51–61.
67 Y. C. Lin, T. C. Chang, Y. J. Tseng, Y. L. Lin, F. J. Huang, F. T. Kung and S. Y. Chang, *Chang Gung Med. J.*, 2000, **23**, 260–266.
68 P. V. Lishko and Y. Kirichok, *J. Physiol.*, 2010, **588**, 4667–4672.
69 M. Riffo, S. Leiva and J. Astudillo, *Int. J. Androl.*, 1992, **15**, 229–237.
70 J. Qiao, H. Zhao, Y. Zhang, H. Peng, Q. Chen, H. Zhang, X. Zheng, Y. Jin, H. Ni, E. Duan and Y. Guo, *Theriogenology*, 2017, **88**, 98–105.
71 D. E. Fullenkamp, L. He, D. G. Barrett, W. R. Burghardt and P. B. Messersmith, *Macromolecules*, 2013, **46**, 1167–1174.
72 S. Schmidt, A. Reinecke, F. Wojcik, D. Pussak, L. Hartmann and M. J. Harrington, *Biomacromolecules*, 2014, **15**, 1644–1652.
73 W. J. Song, P. A. Sontz, X. I. Ambroggio and F. A. Tezcan, *Annu. Rev. Biophys.*, 2014, **43**, 409–431.
74 E. D. Gundelfinger, T. M. Boeckers, M. K. Baron and J. U. Bowie, *Trends Biochem. Sci.*, 2006, **31**, 366–373.
75 W. Maret, *J. Inorg. Biochem.*, 2012, **111**, 110–116.
76 L. Han, M. Monne, H. Okumura, T. Schwend, A. L. Cherry, D. Flot, T. Matsuda and L. Jovine, *Cell*, 2010, **143**, 404–415.
77 M. Monne, L. Han, T. Schwend, S. Burendahl and L. Jovine, *Nature*, 2008, **456**, 653–657.
78 S. Schlafke and A. C. Enders, *J. Anat.*, 1967, **102**, 13–32.
79 R. J. Cole, *J. Embryol. Exp. Morphol.*, 1967, **17**, 481–490.
80 M. Bokhove, K. Nishimura, M. Brunati, L. Han, D. de Sanctis, L. Rampoldi and L. Jovine, *Proc. Natl. Acad. Sci. U. S. A.*, 2016, **113**, 1552–1557.
81 E. Bianchi, B. Doe, D. Goulding and G. J. Wright, *Nature*, 2014, **508**, 483–487.
82 E. Bianchi and G. J. Wright, *Cell cycle*, 2014, **13**, 2019–2020.
83 F. Chimienti, S. Devergnas, A. Favier and M. Seve, *Diabetes*, 2004, **53**, 2330–2337.
84 C. J. Frederickson, S. W. Suh, D. Silva, C. J. Frederickson and R. B. Thompson, *J. Nutr.*, 2000, **130**, 1471S–1483S.
85 R. D. Palmiter, T. B. Cole, C. J. Quaife and S. D. Findley, *Proc. Natl. Acad. Sci. U. S. A.*, 1996, **93**, 14934–14939.
86 S. Yamasaki, K. Sakata-Sogawa, A. Hasegawa, T. Suzuki, K. Kabu, E. Sato, T. Kurosaki, S. Yamashita, M. Tokunaga, K. Nishida and T. Hirano, *J. Cell Biol.*, 2007, **177**, 637–645.
87 P. D. Zalewski, S. H. Millard, I. J. Forbes, O. Kapaniris, A. Slavotinek, W. H. Betts, A. D. Ward, S. F. Lincoln and I. Mahadevan, *J. Histochem. Cytochem.*, 1994, **42**, 877–884.
88 T. Kambe, *Biosci., Biotechnol., Biochem.*, 2011, **75**, 1036–1043.